ELSEVIER

Materials Science and Engineering B 124–125 (2005) 372–375

MATERIALS SCIENCE & ENGINEERING B

www.elsevier.com/locate/mseb

Molecular dynamics characterization of as-implanted damage in silicon

Iván Santos *, Luis A. Marqués, Lourdes Pelaz, Pedro López, María Aboy, Juan Barbolla ✠

Dpto. de Electricidad y Electrónica, Universidad de Valladolid, E.T.S.I. Telecomunicaciones, Campus Miguel Delibes s/n, 47011 Valladolid, Spain

Abstract

We have analyzed the as-implanted damage produced in silicon by B, Si and Ge ions using molecular dynamics (MD) simulations. Implantations were carried out at 50 K to avoid damage migration and annealing. In order to make a statistical study of the damage features, we have simulated hundreds of independent cascades for each ion for the same nuclear deposited energy. We have obtained that the average number of displaced atoms (DA) from perfect lattice positions and the size of defect clusters formed increases with ion mass. This dependence has not been obtained from equivalent binary collisions simulations. This indicates that multiple interactions play an important role in the generation of damage. Amorphous regions are directly formed during the collisional phase of the cascade of Ge and Si ions.
© 2005 Elsevier B.V. All rights reserved.

Keywords: Molecular dynamics; Ion implantation; Radiation damage; Silicon

1. Introduction

The use of solid phase epitaxial growth of amorphous layers generated by ion implantation to achieve highly active and abrupt dopant profiles has revealed the need of predictive amorphization and recrystallization models [1]. One of the difficulties for the development of such models is the lack of an accurate description of the as-implanted damage and its subsequent evolution during thermal annealing. Binary collision approximation (BCA) gives a description of damage in terms of Frenkel pairs, i.e. pairs of interstitials and vacancies. This approach gives reasonable depth profiles and projected ranges of implanted species. An important advantage of BCA is that it is possible to simulate almost every kind of implantation conditions and obtain results with low computational cost [2]. Computer codes such as SRIM [3,4] and MARLOWE [5] are based on that approximation. A more detailed description of the produced damage is provided by molecular dynamics (MD) simulations. Trajectories of ions from BCA and MD simulations are very similar for energies above 200 eV [6]. However, complex defect structures have been observed experimentally [7] and obtained from MD simulations [8–10] but not in BCA simulations. These complex structures or amorphous pockets may play an important role in the amorphization process. However, MD simulations are very CPU time-consuming, which limits the system sizes and times that can be treated. In addition not all simulation conditions are easily obtainable, especially due to the lack of an empirical potential that describes any ion-target system.

In this work, we have used MD to study the collisional phase of ion implantation paying attention to the formation of complex structures. Previous works that also studied ion implantations using MD simulations were limited to one or few cascades [8–10]. Because of the statistical nature of the process a great number of ion-implant simulations are needed to provide a general description of the damage.

2. Simulations

We use classical MD to study the damage produced in crystalline silicon by different types of ions. Implantations are carried out at a simulated temperature of 50 K. At such low temperature damage migration and annealing effects are negligible [10]. Because the ion mass is one of the most relevant parameters for the damage generation we have carried out implants with B, Si and Ge. These ions account for the damage production for low, medium and high mass ions, respectively. The energy of all ions is chosen to be 1 keV. This energy is in the range of practical interest in Si processing and full cascades can be simulated with MD techniques. Energy losses due to the interaction between the ion and the electrons, i.e. the electronic stopping power, are not considered. Thus, the initial energy of ions was completely deposited in the target in the form of nuclear collisions.

Since the projected range of these three ions for the same nuclear deposited energy is different, we considered three com-

* Corresponding author. Tel.: +34 983 42 36 83x5512; fax: +34 983 42 36 75.
E-mail address: ivasan@ele.uva.es (I. Santos).

✠ Recently deceased.

0921-5107/$ – see front matter © 2005 Elsevier B.V. All rights reserved.
doi:10.1016/j.mseb.2005.08.017

putational cells. The dimensions of these cells were estimated using SRIM2003 [4] to contain the full cascade inside: 25 nm × 25 nm × 25 nm in the case of B, 15 nm × 18 nm × 18 nm for Si and 15 nm × 15 nm × 15 nm for Ge. In all cases cells were bounded by (1 0 0) planes in the *X* direction and by (1 1 0) planes in *Y* and *Z* directions. Periodic boundary conditions were only applied in the *Y* and *Z* directions. Ions were implanted with a tilt of 7° respect to the *X*-axis to avoid channeling effects, as it is usually done in the experiments. Atoms of the last two layers in the *X* direction were held fixed and atom velocities of the next four layers were rescaled each time step to maintain the simulated temperature.

Universal ZBL potential [3] was used to describe the ion-target interaction while Tersoff 3 potential [11] was considered to describe the Si–Si bonding interactions. At short distances, Tersoff 3 was splined to the repulsive ZBL potential to better describe the high energy Si–Si interactions.

Under these simulation conditions, we carried out 144 full cascades of Ge, 114 of Si and 121 of B. In the case of B implantation some of the ions (15) were backscattered. These cascades were not considered in the analysis since damage produced was too shallow and thus it was affected by surface effects.

3. Identification of defects

One of the main difficulties that arises when analyzing the generated damage is the identification of defects. There are different criteria for this purpose. An atom can be considered a defect (i) when its potential energy is significantly higher, usually 0.2 eV, than the averaged potential energy of the atoms in the perfect lattice at the simulated temperature [8]; (ii) when it does not have the correct coordination when considering the atomic bonding [12]; or (iii) when it is not in a certain volume centered on lattice sites: small Lindemann spheres [13], Wigner-Seitz cells [14] or spheres with the size of half the nearest-neighbor distance [9]. However, when using these criteria results are affected by the thermal vibration of atoms in the simulation cell. To eliminate thermal vibrations several techniques can be used, such as the cooling down to 0 K or the *steepest-descent/conjugate-gradient* minimization methods [15–17], but they are very computer demanding and cannot be employed to each configuration obtained from the simulation. We have used a method for identifying defects based on the time average of the atom coordinates [18]. This method eliminates atom vibrations and can be applied during the actual MD simulation. It has been successfully applied before to study recrystallization processes in silicon [19] and the configurational and energetic properties of the Si self-interstitial [18].

We consider that the collisional phase of a cascade has finished when the cell has been thermalized, i.e. when the energy has been spread out over all the atoms in the cell. The simulation continues over 1000 time steps during which atom positions are averaged in time. Then we compare the 'averaged' atom positions with the perfect lattice before being implanted, i.e. the lattice sites. When an atom is closer than 0.07 nm to a lattice site, the atom is associated with that site. Empty sites (ES) appear when a lattice site does not have any atom associated to it, and displaced atoms (DA) when an atom has not been associated to any lattice site. However, in highly disordered regions where lattice order is completely lost, atoms may happen to be close to a lattice site and therefore be associated to it. However, these atoms should not be considered as atoms in a perfect lattice position. To avoid these situations we also considered displaced atoms those ones that being associated to a lattice site have more than two displaced nearest neighbors. Once DA and ES are identified, they are grouped. The distance used to group them was the corresponding to the first minimum of the radial distribution function $g(r)$ for amorphous Si at 300 K [19] which is 0.285 nm.

Table 1
Summary of the results obtained from our MD simulations: average number of DA generated, mean maximum defect size and mean defect size (number of DA) and percentage of DA in defects for different type of defects

	BORON	SILICON	GERMANIUM
Average number of DA	68	89	130
Mean defect size	8.6	22.2	63.5
Mean maximum defect size	14.9	32.2	80.9
MD			
Point defects (%)	38.19	25.25	12.53
Defects with 10 DA or less (%)	45.15	33.36	19.26
Defects with $10 < DA \leq 50$ (%)	14.93	29.18	16.98
Defects with $50 < DA$ (%)	1.73	12.21	51.23
SRIM			
Incident energy (keV)	1.5	1.2	1.1
Frenkel pairs	35	35	35

There are also shown the implantation conditions of the equivalent SRIM simulations (energy of the implanted ion) and the number of Frenkel pairs produced. In these simulations the displacement energy was 15 eV.

4. Results and discussion

We have studied the number of DA and ES produced by the ions considered. These values along with other data obtained from our MD simulations are shown in Table 1. The average number of DA is 68 for B, 89 for Si and 130 for Ge. The distribution of cascades as a function of their number of DA is represented in Fig. 1. For the ions simulated in this work,

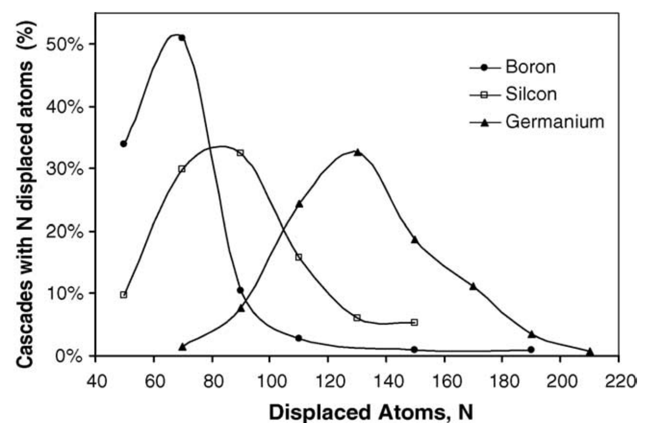

Fig. 1. Percentage of cascades with a certain number of DA. In order to have a representative plot we have made equal intervals of 20 units in the number of displaced atoms.

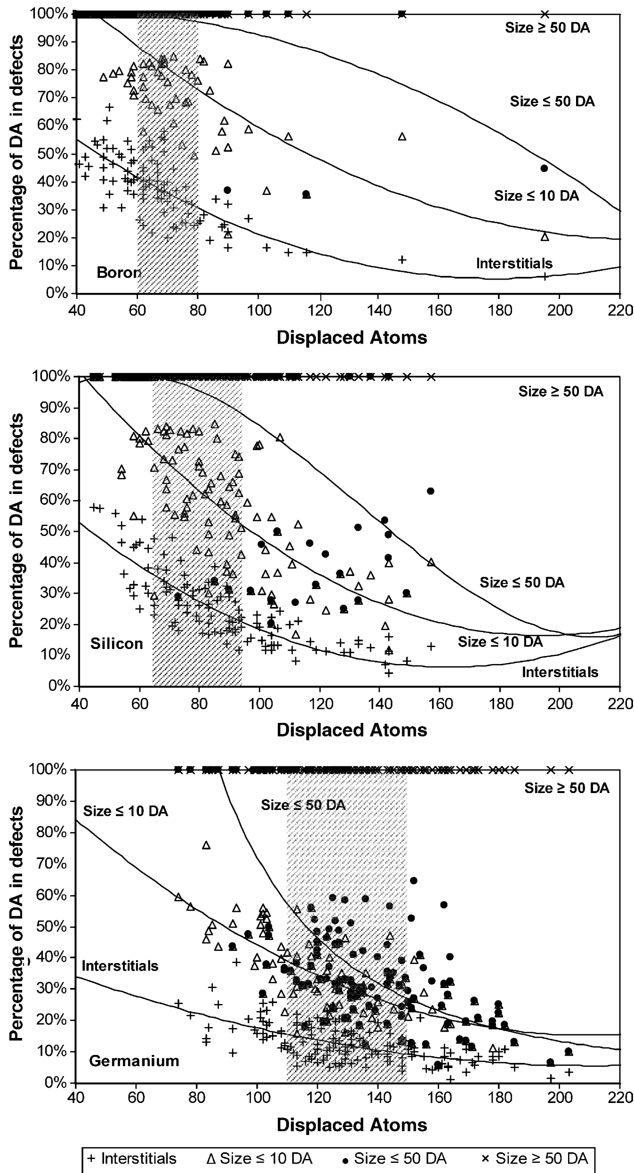

Fig. 2. Distribution of displaced atoms in defects as a function of the displaced atoms of each cascade. Solid lines correspond to a fit of the data to a polynomial expression. Regions corresponding to the average behavior of each ion are shown as shadowed.

the number of DA increases linearly with ion mass. It can be observed that the curve of the distribution of cascades presents a maximum around the average number of DA for each ion.

The presence of a clear maximum in the curves indicates that most of the cascades produce a number of DA similar to the average for each ion. However, there are cascades with a behavior very different from the average. These singular cascades may be misleading when trying to give a general description of the damage generated by a specific ion if not enough statistics is provided.

The next step in our analysis is to characterize the morphology of the produced damage. In Fig. 2, we show the accumulative percentage of DA in defects of different sizes: point defects, small clusters (DA $\leq$ 10), medium-size defects (DA $\leq$ 50), and big defects (DA > 50). A common trend is observed for the three

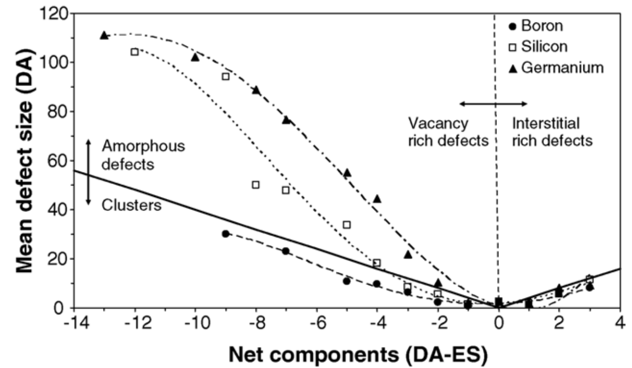

Fig. 3. Mean defect size as a function of the net components in the defect. Dashed lines correspond to a fit of the data to a polynomial expression. Solid line has a slope of 4 and separate regions of defect clusters (below) and amorphous defects (above). Regions of interstitial and vacancy rich defect clusters are also shown.

ions: the larger the number of DA produced in a given cascade, the bigger the defects and the larger the percentage of DA in big defects. However, there are notable differences between the average morphology of damage generated for the three ions. It can be observed that as the ion mass increases, the percentage of DA in point defect and small defect clusters decreases while the percentage of DA in big defect clusters increases. In the case of B, most cascades produce isolated interstitials and small defect clusters, being the mean defect size of only 8.6 DA. In the case of Ge, more than 50% of DA are part of big defects clusters, being the mean defect size of 63.5 DA. For Si about 60% of DA belong to small or medium defect clusters with a mean defect size of 22.2 DA. Thus, we quantitatively confirm that damage generated by light ion implantations is mostly in the form of point defects and small clusters while the damage generated by heavy ion implantations is formed by big defect clusters in agreement with Ref. [9].

Another point of interest in this analysis is the atomic balance in defect clusters, i.e. their net components (number of DA minus number of ES). This is an important information since upon thermal annealing, DA and ES recombine among them leaving only the unbalanced atoms in the lattice, which control the dopant diffusion. It is interesting to note that some defect structures can be assigned to different values of DA and ES but with the same net value. For instance, the simplest configuration of the Si self-interstitial consists of one DA and none ES (tetrahedral interstitial, [18]) but there are other configurations that having a net value DA − ES = 1 are associated to other DA and ES values (dumbbell interstitial: 2 DA − 1 ES, extended interstitial: 4 DA − 3 ES, [18]). When the net value is larger than one, we can assign these defects to clusters (di-interstitials, divacancies, etc.). However, not all damage can be simplified to its net components. For instance, a defect with 19 DA and 20 ES cannot be considered as a vacancy but rather as an amorphous region with an unbalanced atom. In order to distinguish between defect clusters and amorphous defects we have considered a criterion based on the extended interstitial case: if the ratio DA/(DA − ES) is larger than 4, defects are considered as amorphous damage, and as defect clusters otherwise. In Fig. 3, we represent the mean defect size as a function of its net com-

ponent for the three ions. We have also marked a line with slope 4 that separates the amorphous damage from clusters or point defects. It can be seen that interstitial rich defects are relative small and all of them can be considered as interstitial clusters with similar sizes for all ions. Vacancy rich defects are different for each ion. In the case of B, all of them can be considered as small vacancy clusters, while most of the damage generated by Ge and Si can be considered as amorphous regions.

In order to compare our MD results with the damage generated using BCA, we have used SRIM2003 [4] to obtain the number of Frenkel pairs produced by the ions under study. As in this BCA code electronic stopping power is taken into account, the initial energy of the ions has been scaled to keep the deposited energy in nuclear collisions equal to 1 keV in the three cases as indicated in Table 1. The number of Frenkel pairs obtained is the same independently of the ion mass. Although these results are not directly comparable with the number of DA obtained in our MD simulations, the fact that the ion mass dependence appears in our MD simulations and not in SRIM calculations is a clear evidence that for this range of energy multiple interactions – included in the empirical potential used in MD and not in the BCA approximation – play an important role in the generation of defects and therefore in the amorphization process.

5. Conclusions

We have analyzed the as-implanted damage produced in silicon by B, Si and Ge ions using MD simulations. The averaged number of DA increases linearly with ion mass and from our statistical study we conclude that most of the cascades produce a number of DA close to the average for each ion. This dependence with ion mass has not been found in equivalent BCA simulations, which indicates that for this range of energy, multiple interactions play an important role in the generation of defects and therefore in the amorphization process.

As the ion mass increases, the percentage of DA in point defect and small defect clusters decreases while the percentage of DA in big defect clusters increases. In general the larger the number of DA produced in a given cascade, the bigger the defects and the larger the percentage of DA in big defects. Interstitial rich defects formed during the collisional phase are relative small. Amorphous regions formed with Si and Ge are vacancy rich.

Acknowledgements

This work has been supported by the Spanish D.G.I.C.Y.T. under project BFM 2001–2250 and the J.C.yL. Conserjería de Educación y Cultura under project VA070A05.

References

[1] International Technology Roadmap for Semiconductors, http://public.itrs.net/.
[2] J.M. Hernández-Mangas, J. Arias, L. Bailón, M. Jaraíz, J. Barbolla, J. Appl. Phys. 91 (2002) 658.
[3] J.F. Ziegler, The Stopping and Ranges of Ions in Matter, vol. 1, Pergamon, New York, 1977.
[4] http://www.srim.org.
[5] M.T. Robinson, I.M. Torrens, Phys. Rev. B 9 (1974) 5008.
[6] M. Jaraíz, G.H. Gilmer, D.M. Stock, T. Diaz de la Rubia, Nucl. Instrum. Methods Phys. Res. B 102 (1995) 180.
[7] S.E. Donnelly, R.C. Birtcher, V.M. Visnyakov, G. Carter, Appl. Phys. Lett. 82 (2003) 1860.
[8] T. Diaz de la Rubia, G.H. Gilmer, Phys. Rev. Lett. 74 (1995) 2507.
[9] M.J. Caturla, T. Diaz de la Rubia, L.A. Marqués, G.H. Gilmer, Phys. Rev. B 54 (1996) 16683.
[10] K. Nordlund, M. Ghaly, R.S. Averback, M.J. Caturla, T. Diaz de la Rubia, J. Tarus, Phys. Rev. B 57 (1998) 7556.
[11] J. Tersoff, Phys. Rev. B 38 (1988) 9902.
[12] M. Tang, L. Colombo, J. Zhu, T. Diaz de la Rubia, Phys. Rev. B 55 (1997) 14279.
[13] H. Hensel, H.M. Urbassek, Phys. Rev. B 58 (1998) 4756.
[14] J.B. Gibson, A.N. Goland, M. Milgram, G.H. Vineyard, Phys. Rev. 120 (1960) 1229.
[15] H.R. Shober, Phys. Rev. B 39 (1989) 13013.
[16] L.J. Munro, D.J. Wales, Phys. Rev. B 59 (1999) 3969.
[17] G.H. Gilmer, T. Diaz de la Rubia, D.M. Stock, M. Jaraíz, Nucl. Instrum. Methods Phys. Res. B 102 (1995) 247.
[18] L.A. Marqués, L. Pelaz, P. Castrillo, J. Barbolla, Phys. Rev. B 71 (2005) 085204.
[19] L.A. Marqués, M.J. Caturla, T. Diaz de la Rubia, G.H. Gilmer, J. Appl. Phys. 80 (1996) 6160.